TRIM28 is a transcriptional activator of the mutant TERT promoter in human bladder cancer

Neeraj Agarwal[a,b], Sebastien Rinaldetti[c], Bassem B. Cheikh[d], Qiong Zhou[c], Evan P. Hass[e,f], Robert T. Jones[g], Molishree Joshi[h], Daniel V. LaBarbera[c], Simon R. V. Knott[d], Thomas R. Cech[e,f,i], and Dan Theodorescu[b,j,1]

[a]Department of Medicine, Cedars-Sinai Medical Center, Los Angeles, CA 90048; [b]Cedars-Sinai Samuel Oschin Comprehensive Cancer Institute, Los Angeles, CA 90048; [c]Skaggs School of Pharmacy and Pharmaceutical Sciences, University of Colorado Anschutz Medical Campus, Aurora, CO 80045; [d]Department of Biomedical Sciences, Cedars-Sinai Medical Center, Los Angeles, CA 90048; [e]Department of Biochemistry, University of Colorado, Boulder, CO 80303; [f]BioFrontiers Institute, University of Colorado, Boulder, CO 80303; [g]Department of Pharmacology, University of Colorado School of Medicine, Aurora, CO 80045; [h]Functional Genomics Facility, University of Colorado Anschutz Medical Campus, Aurora, CO 80045; [i]HHMI, University of Colorado, Boulder, CO 80303; and [j]Department of Surgery, Cedars-Sinai Medical Center, Los Angeles, CA 90048

Edited by Webster K. Cavenee, Ludwig Institute for Cancer Research Ltd, La Jolla, CA, and approved June 30, 2021 (received for review February 6, 2021)

Bladder cancer (BC) has a 70% telomerase reverse transcriptase (TERT or hTERT in humans) promoter mutation prevalence, commonly at −124 base pairs, and this is associated with increased hTERT expression and poor patient prognosis. We inserted a green fluorescent protein (GFP) tag in the mutant hTERT promoter allele to create BC cells expressing an hTERT-GFP fusion protein. These cells were used in a fluorescence-activated cell sorting–based pooled CRISPR-Cas9 Kinome knockout genetic screen to identify tripartite motif containing 28 (TRIM28) and TRIM24 as regulators of hTERT expression. TRIM28 activates, while TRIM24 suppresses, hTERT transcription from the mutated promoter allele. TRIM28 is recruited to the mutant promoter where it interacts with TRIM24, which inhibits its activity. Phosphorylation of TRIM28 through the mTOR complex 1 (mTORC1) releases it from TRIM24 and induces hTERT transcription. TRIM28 expression promotes in vitro and in vivo BC cell growth and stratifies BC patient outcome. mTORC1 inhibition with rapamycin analog Ridaforolimus suppresses TRIM28 phosphorylation, hTERT expression, and cell viability. This study may lead to hTERT-directed cancer therapies with reduced effects on normal progenitor cells.

CRISPR-Cas9 KnockIn | hTERT | promoter mutation | Kinome KO screening

A hallmark of cancer is replicative immortality, commonly driven by the reactivation of telomerase reverse transcriptase (TERT or hTERT in humans), the catalytic subunit of telomerase, which is responsible for telomere maintenance (1, 2). In contrast to other components of the telomerase complex, hTERT has low expression in human stem and germ cells and is undetectable in most adult somatic tissues (2). Telomerase reactivation/reexpression is observed in nearly 90% of cancers and results from the transcriptional up-regulation of hTERT (2, 3). hTERT also has "extratelomeric" functions including driving cell proliferation, DNA damage signaling, and protection of cancer cells from apoptosis (4–7). These and its telomeric functions probably explain why hTERT expression is associated with poor patient outcomes in many cancer types (8–11). Two hot spot point mutations in the hTERT promoter at 124 (C228T) and 146 (C250T) base pairs (bp) upstream of the translation start site comprise 96.3% of all hTERT promoter mutations. These are present in 70% of bladder cancers, 67% of glioma, 60% of thyroid cancer, and 49% of melanomas (12). These are found in 43 principal cancer types (12) and are associated with increased promoter activity, gene transcription, telomerase activity, stable telomere length (8, 13, 14), and poor patient prognosis (8, 9, 15–18).

Targeted therapies toward telomerase inhibition based on targeting either hTERT activity or its RNA subunit with small-molecule inhibitors or antisense oligonucleotides have been developed, yet none has been broadly successful in the clinical arena (19). Imetelstat, a telomerase inhibitor, was the first such agent in clinical use and has had mixed clinical results (20). Studies on patients with non-small cell lung cancer (NSCLC) showed only limited efficacy, (21) and in pediatric brain tumors, the drug was only able to be administered for an average of 13 d before intolerable hematologic toxicity occurred (22). The use of "drug holidays" to mitigate such toxicities led to the reestablishment of telomere length and continued cell growth (19, 23). Since telomerase is expressed in hematologic stem cells, these findings highlight the limitations of current approaches.

The finding that several cancers have a high occurrence of hTERT promoter mutations offers a novel therapeutic angle that has the potential to be cancer specific. This is important given the issues with telomerase inhibition mentioned above and because wild-type hTERT is also expressed in some normal tissues (https://www.gtexportal.org/home/gene/TERT). hTERT expression is regulated by factors such as c-Myc (24), NF-κB(25), and β-catenin (26). We and others found the multimeric ETS factor GABPA/B1 preferentially regulates mutant promoter-driven hTERT reactivation in cancer models (27–30). However, GABPA is not a

Significance

Telomerase reverse transcriptase (hTERT) is involved in immortalization and survival of cancer cells. Recurring mutations in its promoter often lead to its reexpression in cancer. Therapies targeting hTERT activity have been challenging to develop, and none are in routine use. Using targeted functional genomics knockout screening in a human bladder cancer model, we found that transcription factor TRIM28 activates hTERT expression preferentially from the mutant promoter allele. We also revealed a therapeutically targetable mechanism whereby mTORC1-mediated phosphorylation of TRIM28 is required to activate hTERT transcription. This study describes an approach to functional screening of endogenous promoters and insights into TERT regulation, and it may aid clinicians in making informed decisions for precision therapy of cancer patients harboring hTERT promoter mutations.

Author contributions: N.A. and D.T. designed research; N.A., S.R., B.B.C., Q.Z., E.P.H., and R.T.J. performed research; N.A., D.V.L., S.R.V.K., T.R.C., and D.T. analyzed data; S.R. and Q.Z. conducted high-content imaging, three-dimensional assays, and did the clinical analysis of the TCGA dataset; B.B.C. performed analysis for CRISPR knockout screening and RNA-seq data; E.P.H. did Southern blotting for telomere length; R.T.J. helped with CRISPR screening; M.J. designed and generated plasmids for CRISPR-Cas9 knock in; D.V.L. and T.R.C. supervised parts of the study and extensively reviewed the manuscript; S.R.V.K. performed analysis for CRISPR knockout screening and RNA-seq data and supervised parts of the study and extensively reviewed the manuscript; D.T. initiated the project, generated research funds and ideas, and directed and coordinated the project; and N.A. and D.T. wrote the paper.

Competing interest statement: T.R.C. is on the board of directors of Merck, Inc. and a scientific advisor to Storm Therapeutics and Eikon Therapeutics.

This article is a PNAS Direct Submission.

[1]To whom correspondence may be addressed. Email: dan.theodorescu@cshs.org.

This article contains supporting information online at https://www.pnas.org/lookup/suppl/doi:10.1073/pnas.2102423118/-/DCSupplemental.

Published September 13, 2021.

tractable therapeutic target in cancer (31–33), motivating us to search for druggable pathways and targets that regulate mutant hTERT. Here, we developed a high-throughput platform to functionally probe endogenous hTERT transcription and identify genetic factors and signaling pathways specifically regulating mutant promoter-driven hTERT reactivation. We used a human kinase knockout library for screening, as kinases are druggable and phosphorylation is often associated with transcriptional regulation (34, 35).

Results

Generation and Characterization of Endogenous GFP-hTERT–Expressing Cells. Most human bladder cancers (36) and cell lines (8) have a heterozygous C > T mutation in the promoter region of hTERT, −124 bp from the translation start site. The UMUC3 human bladder cancer cell line has this heterozygous mutation and expresses hTERT messenger RNA (mRNA) and protein (8). Therefore, we used this line to knock in an enhanced green fluorescent protein (GFP) tag at a wild-type (WT) or mutant hTERT promoter allele, using the CRISPR-Cas9 technique as illustrated in Fig. 1*A*. This allowed us to monitor promoter activity from either allele in different subclones of the same parental cell line.

One clone each for an enhanced GFP tag knock in at WT and mutant hTERT alleles passed the screening and were named UWG6 and UMG12, respectively (Fig. 1 *B* and *C* and *SI Appendix*, Fig. S1*A*). Further characterization was done after sorting these clones for GFP^{High} cells (*SI Appendix*, Fig. S1*B*). Since UMUC3 is a hyper-triploid cell line, we checked the hTERT copy numbers in the parental line and subclones. Both clones have a similar distribution of hTERT copies as the parental UMUC3 cell line with most cells having four copies (*SI Appendix*, Fig. S2*A*). UMG12 expresses GFP-hTERT mRNA and protein at higher levels than UWG6 (Fig. 1*D* and *SI Appendix*, Fig. S2*B*). The additional free GFP protein band is most likely a degradation product or nonspecific (*SI Appendix*, Fig. S2 *B* and *C*). As further validation, the treatment of clones with hTERT small interfering RNA (siRNA) reduced the levels of GFP-hTERT fusion protein (Fig. 1*E*), and GFP single guide RNA (sgRNA) reduced both hTERT and GFP mRNA levels (Fig. 1*F*). The more modest effect of GFP sgRNA on total hTERT mRNA than on GFP mRNA is consistent with the cell lines containing both GFP-edited and unedited hTERT alleles. This also explains why the total hTERT mRNA levels in both clones are similar to those of the parental UMUC3 cell line (*SI Appendix*, Fig. S2*D*), even though the GFP-tagged hTERT has substantially higher expression in UMG12 cells.

We also studied the cellular localization of GFP-hTERT in both clones and found that GFP-hTERT protein resides in the nucleus, consistent with reported nuclear localization of hTERT (37, 38) (Fig. 1*G*). UMG12 maintains baseline GFP expression in 82 to 94% of cells over 100 d in culture, while in the UWG6 clone GFP expression is reduced to 41 to 59% of cells over time (Fig. 1*H* and *SI Appendix*, Fig. S2*E*). Since GABPA is reported to specifically bind to and enhance hTERT expression from the mutant promoter allele, we knocked down GABPA in UMG12 cells and observed reduced hTERT, GFP, and GFP-hTERT mRNA levels (*SI Appendix*, Fig. S2*F*). Furthermore, to confirm telomerase activity is unaffected by the GFP-hTERT fusion, we cultured UWG6, UMG12, and UMUC3 cells for 5 wk and performed telomeric restriction fragment length analysis on each line. UWG6 and UMG12 cells showed stable telomere lengths (*SI Appendix*, Fig. S2*G*). Even though each subline has its own telomere length distribution, the maintenance of telomere length over time indicates no effect of GFP-hTERT fusion on telomerase activity. These results confirm that GFP has successfully tagged either an endogenous mutant or WT hTERT promoter allele in UMG12 and UWG6, respectively. These results also established the UMG12 clone as a reliable model for doing functional genomic screening to identify regulators of hTERT reactivation from the mutant promoter allele.

Identifying Kinases Involved in hTERT Regulation. To identify regulators of mutant promoter-driven hTERT expression, we performed screening using the Brunello Human Kinome CRISPR knockout pooled library (39) in UMG12 cells. To identify promoter mutant hTERT regulators, we compared sgRNA proportions in cells that had lost or gained GFP-hTERT expression with those in unsorted or GFP^{Medium}-sorted populations (Fig. 2*A*). We choose the earliest possible time points of 2 and 4 d post-selection based on the dynamics of GFP knockdown with a GFP-specific sgRNA (*SI Appendix*, Fig. S3*A*). This reduced the probability of false positives or negatives resulting from an essentiality effect. Profiling the two time points 2 d apart also helped identify targets with different knockdown dynamics. The quality of the screening data was good, with 63 to 68% mapped reads, a negligible level of sgRNA dropout from initial pools, and an even distribution of total sgRNA counts in all samples (*SI Appendix*, Fig. S3 *B–D*). Using the highly rigorous MAGeCK-VISPR (Model-based Analysis of Genome-wide CRISPR/Cas9 Knockout—VISualization of crisPR screens) algorithm, we searched for sgRNAs and corresponding genes that were enriched or depleted in the sorted populations (40, 41). sgRNAs for genes activating hTERT expression should be enriched in GFP^{Low} cells and lost in GFP^{High} cells and vice versa for genes suppressing hTERT expression. We also sorted and sequenced cells with medium GFP intensity (GFP^{Medium}) as a negative control. To select the statistically significant regulators of hTERT, we used the criteria of genes whose knockout caused the cells to move toward either the GFP^{Low} or GFP^{High} side with enrichment of sgRNAs with the false discovery rate (FDR) ≤ 0.01 in one population and depletion with FDR ≤ 0.01 in the opposite population as compared to unsorted cells at day 2 and/or day 4. Tripartite motif containing 28 (TRIM28), a member of the TRIM family of proteins mainly known for its activity as a transcription regulator, was significantly enriched in GFP^{Low} cells at day 2 with more enrichment on day 4. In contrast, the same sgRNAs were lost in GFP^{High} cells (Fig. 2 *B* and *C* and *SI Appendix*, Fig. S4). sgRNAs for another TRIM family member, TRIM24, were enriched in GFP^{High} cells and lost in GFP^{Low} cells both at day 2 and 4 (Fig. 2 *B* and *C* and *SI Appendix*, Fig. S4). Importantly, none of the 100 nontargeting control (NTC) sgRNAs survived this criterion at both time points (*SI Appendix*, Figs. S4 and S5). Interestingly, our screening strategy revealed two members of the same family, TRIM28 and TRIM24, as regulators of hTERT expression from the mutant promoter.

TRIM28 Is an Activator and TRIM24, a Suppressor of hTERT. To validate our findings and to determine their specificity for the mutant promoter, we transiently knocked down TRIM28 and TRIM24 using pools of four siRNAs in UMG12 and UWG6 clones. TRIM28 was depleted by more than 90% in both clones (Fig. 3*A*) and resulted in decreased GFP-hTERT mRNA in UMG12 cells only (Fig. 3*B*). TRIM24 was also efficiently depleted by about 80% in both clones with siRNA knockdown (Fig. 3*C*). TRIM24 knockdown increased GFP-hTERT mRNA in UMG12 cells only (Fig. 3*D*). These results were further strengthened by observing similar changes in GFP-hTERT fusion protein levels. GFP-hTERT protein levels were also decreased in TRIM28-silenced UMG12 cells and increased in TRIM24-silenced UMG12 cells (Fig. 3*E*). Neither TRIM28 nor TRIM24 silencing had any impact on GFP-hTERT protein levels in UWG6 cells (Fig. 3*F*). Furthermore, three other established bladder cancer cell lines with −124C > T mutation showed decreased hTERT mRNA levels following highly efficient TRIM28 knockdown, while two bladder cancer cell lines harboring the WT promoter showed no change (Fig. 3 *G* and *H*). TRIM24 knockdown induced significant

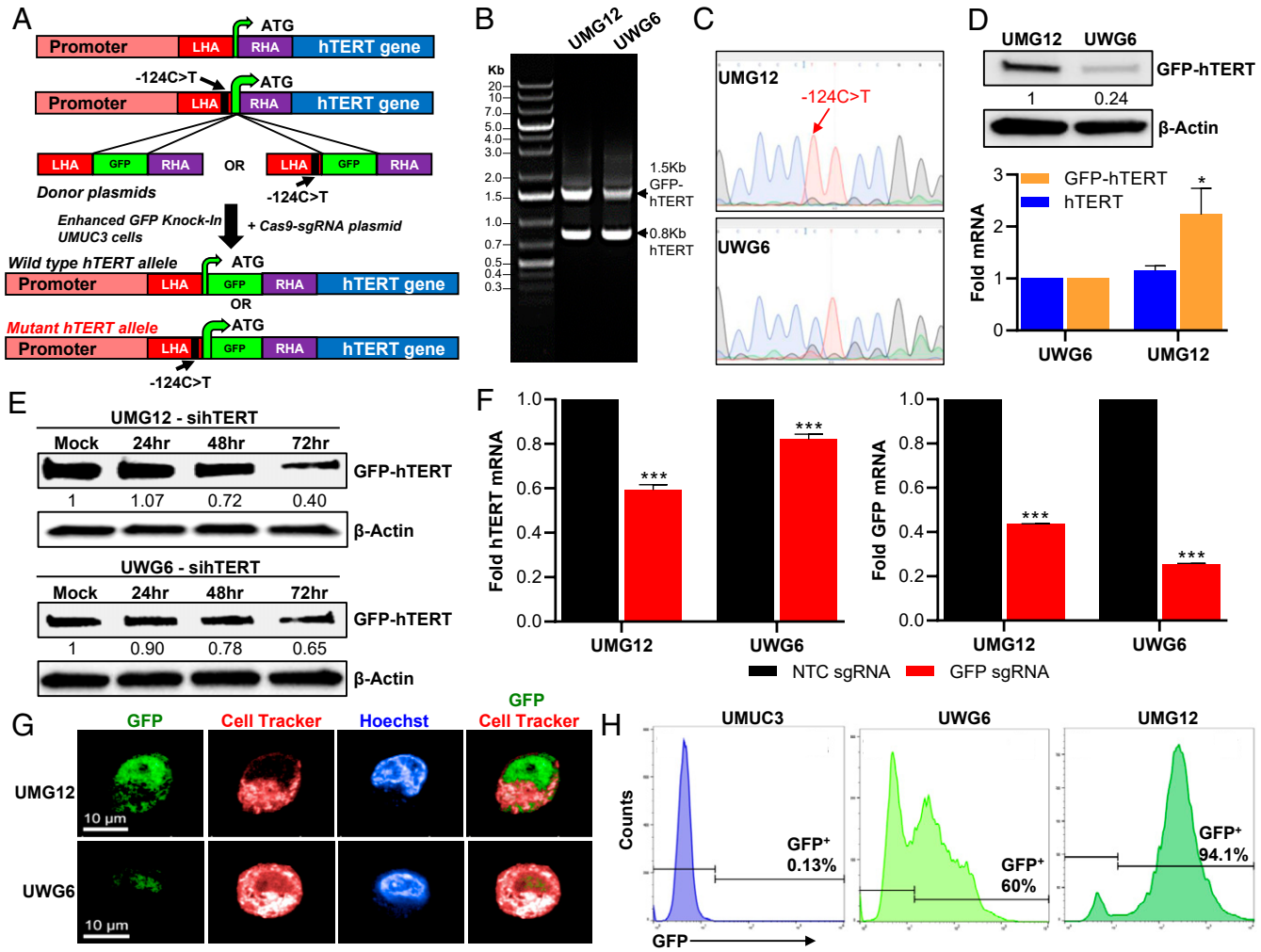

Fig. 1. Allele-specific CRISPR-Cas9 mediated knock in of enhanced GFP at endogenous hTERT promoter alleles. (*A*) Schematic diagram of knockin strategy. LHA: left homology arm, RHA: right homology arm. (*B*) PCR to verify successful tagging of GFP to hTERT in selected clones. UMG12–GFP tag at mutant promoter allele, UWG6–GFP tag at WT promoter allele. Also reference *SI Appendix*, Fig. S1*A*. (*C*) 1.5-Kb GFP-hTERT band was gel purified and Sanger sequenced to confirm tagging at either allele. (*D*) Protein expression of GFP-tagged hTERT in UMG12 and UWG6 clones detected by anti-GFP antibody and mRNA expression by qRT-PCR. Also reference *SI Appendix*, Fig. S2 *B–D*. (*E*) Transient knockdown of hTERT by siRNA. Levels of GFP-hTERT detected by anti-GFP antibody are shown. (*F*) GFP sgRNA-mediated KD of GFP-hTERT as measured by qRT-PCR for hTERT and GFP. NTC sgRNA was used as control for comparison. Bars represent mean ± SEM, $n = 3$ from independent experiments. *P value < 0.05; ***P value < 0.001. (*G*) 63× water images of clones. Cell tracker and Hoescht 33342 were used to stain the cytoplasm and nuclei, respectively. (*H*) GFP histograms for UMG12 and UWG6 cells by FACS showing GFP intensity distribution among cells within each clone at 100 d (time course shown in *SI Appendix*, Fig. S2*E*). UMUC3 is a parental cell line used to adjust the gates for unstained cells.

hTERT mRNA increases in most cell lines with the mutation, while cells harboring the WT promoter were unaffected (Fig. 3 *I* and *J*). Similar regulation of hTERT by TRIM28 and TRIM24 was also observed in glioblastoma and melanoma cell lines harboring −124C > T mutation (*SI Appendix*, Fig. S6 *A–D*). These results validate and establish TRIM28 and TRIM24 as regulators of hTERT expression from the mutant hTERT promoter in cancer cell lines that do not harbor the GFP-tagged hTERT gene.

Biological and Clinical Relevance of the Relationship between TRIM28 and hTERT. We have shown that high hTERT expression is correlated with reduced disease-specific survival in human bladder cancer (8). TRIM28 is also significantly up-regulated in cancer and correlates with worse patient survival (42). To understand the effect of inhibiting TRIM28 and hTERT on cancer cell growth, we knocked down both mRNAs in different cell lines (Fig. 3*G* and *SI Appendix*, Fig. S6*E*) and observed a short-term reduction in proliferation at similar levels in most cell lines regardless of hTERT promoter mutation status (Fig. 4*A*). We also observed the short-term inhibition in growth of melanoma and glioblastoma cell lines as well with TRIM28 and hTERT knockdown (*SI Appendix*, Fig. S6 *A*, *E*, and *F*). Moreover, hTERT overexpression was able to partially rescue the cell growth inhibition in UMUC3 cells transiently depleted of TRIM28 (Fig. 4*B* and *SI Appendix*, Fig. S6 *G* and *H*).

To study growth in vivo, we produced TRIM28 and hTERT knockdown lines by transducing lentivirus harboring corresponding sgRNAs and a nontargeting control in UMUC3 cells. TRIM28 and hTERT depletion were confirmed before inoculating the cells in mice (*SI Appendix*, Fig. S6*I*). When these cells were subcutaneously injected into immune-compromised hosts, we observed significantly decreased tumor growth with both hTERT and TRIM28 depletion (Fig. 4*C*). We also plotted the survival curve with tumors reaching the Institutional Animal Care and Use Committee (IACUC) size limit as the cause of death and observed modestly significant better survival with TRIM28 and hTERT

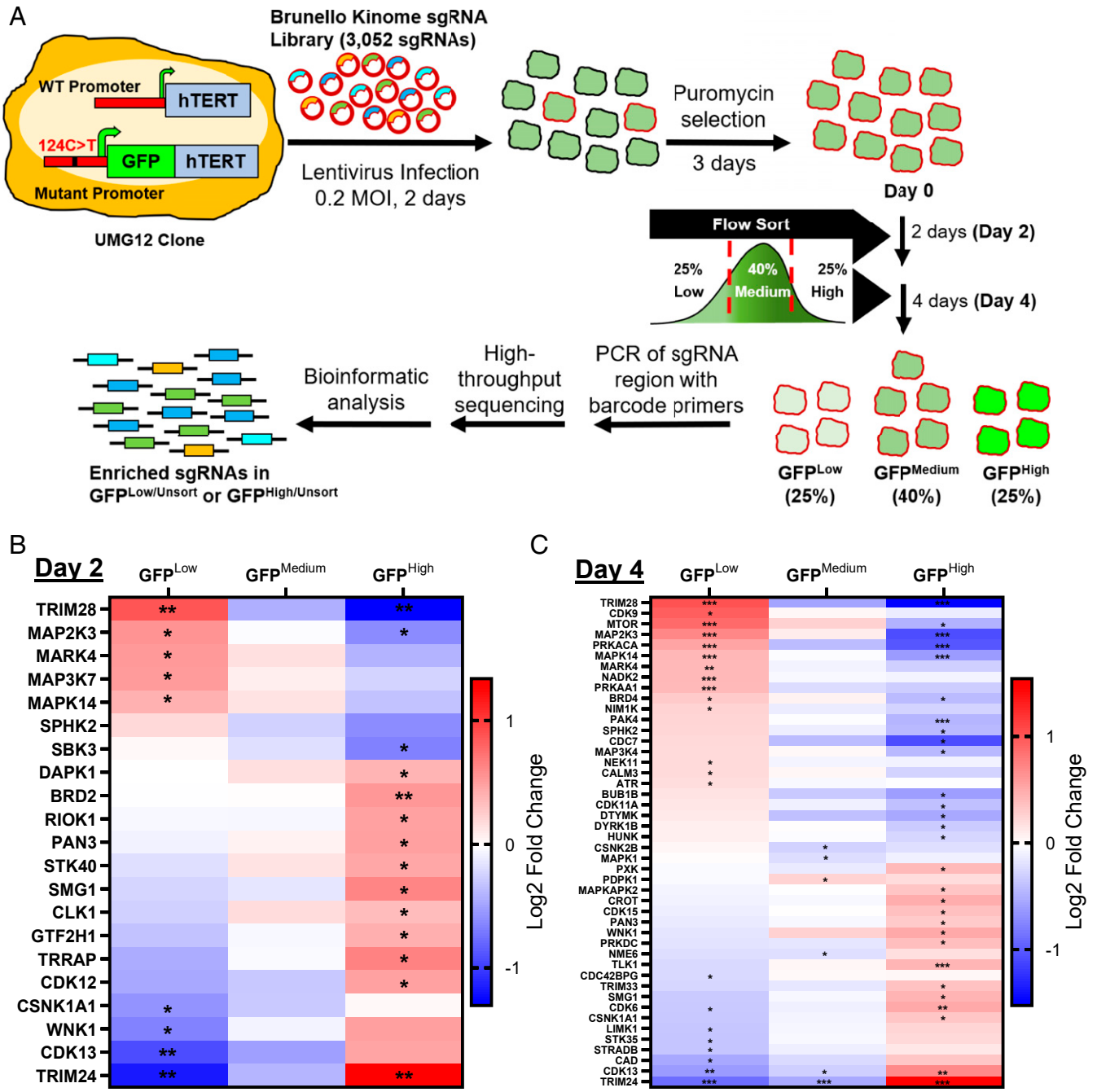

Fig. 2. Kinome KO functional genomic screening by monitoring GFP-hTERT expression from mutant promoter allele. (*A*) Schematic diagram of workflow for screening. (*B* and *C*) Heat maps showing genes with altered sgRNAs in flow-sorted cell populations as indicated compared to unsorted UMG12 cells transduced with library lentivirus. *FDR < 0.1; **FDR < 0.01; ***FDR < 0.001. Also reference *SI Appendix*, Figs. S3–S5.

knockdown (KD) compared to control mice (Fig. 4*D*). The median survival for control mice was 31 d, while for TRIM28 and hTERT KD mice was 42 d.

To evaluate the clinical relevance of TRIM28 as an activator of hTERT, we analyzed the correlation between hTERT and TRIM28 expression in bladder cancer, melanoma, and glioblastoma, which have a high frequency of hTERT promoter mutations. In agreement with our experimental findings, hTERT and TRIM28 are positively correlated in all three cancer types (Fig. 4*E* and *SI Appendix*, Fig. S6 *J* and *K*). Furthermore, through an examination of the TCGA data, we found that TRIM28 expression is associated with poor survival in bladder cancer (Fig. 4*F*) and melanoma (*SI Appendix*, Fig. S6*L*). Interestingly, comparing expression of both hTERT and TRIM28 in bladder cancer subtypes, we observed higher expression in the more aggressive neuroendocrine bladder cancer subtype, although the number of patients is relatively low (*SI Appendix*, Fig. S6 *M* and *N*).

TRIM28 and TRIM24 Interact and Are Recruited to Mutant hTERT Promoters. To determine how TRIM28 and TRIM24 regulate hTERT, we performed KDs of both genes (*SI Appendix*, Fig. S7 *A* and *B*) and analyzed hTERT mRNA levels in different cell

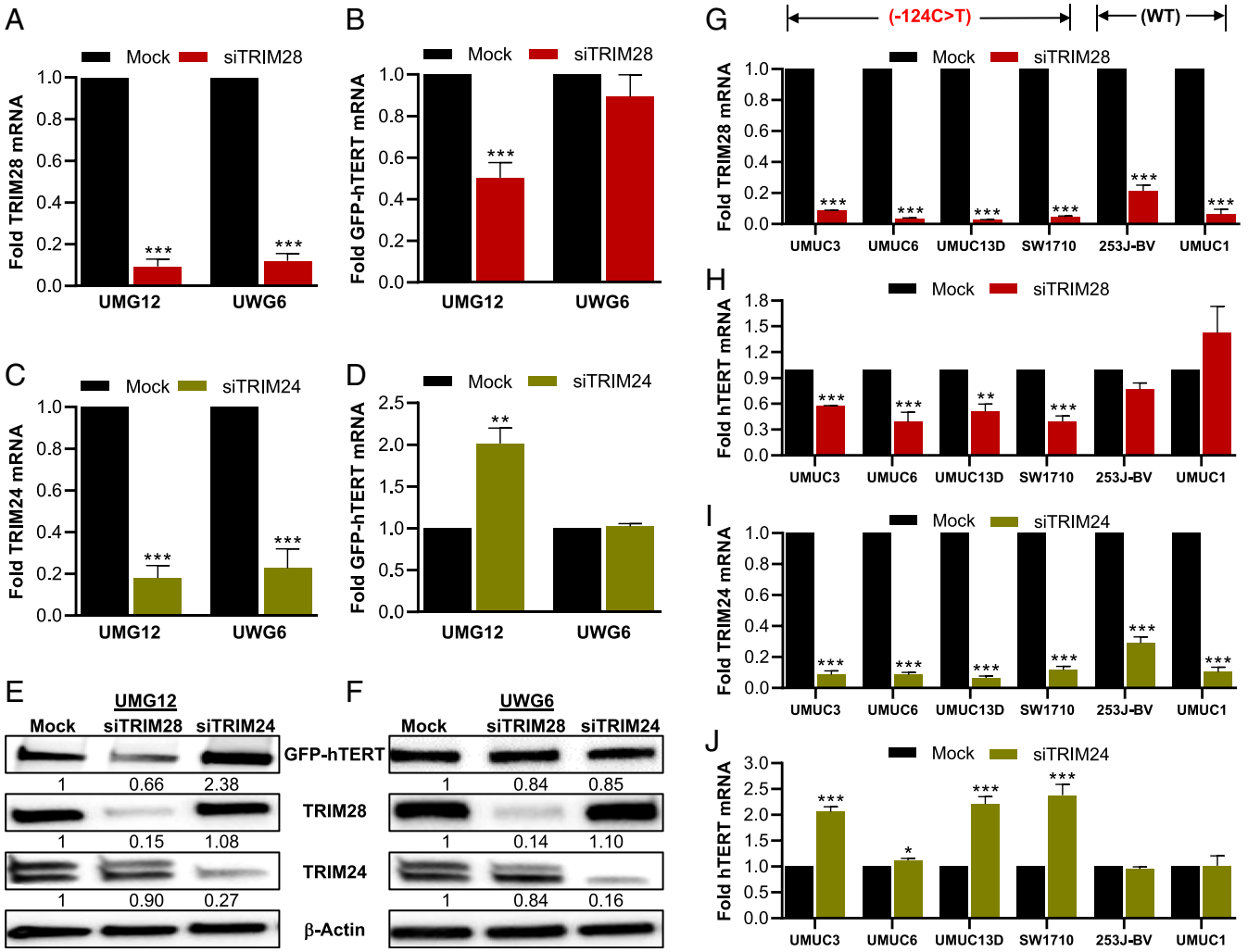

Fig. 3. TRIM28 and TRIM24 are regulators of hTERT expression from the mutant promoter allele. After transient KD of TRIM28 with smartpool siRNA for 72 h in UMG12 and UWG6 cells, mRNA levels of (*A*) TRIM28 and (*B*) GFP-hTERT were measured by qRT-PCR. After transient KD of TRIM24 with smartpool siRNA for 72 h in UMG12 and UWG6 cells, mRNA levels of (*C*) TRIM24 and (*D*) GFP-hTERT were measured by qRT-PCR. (*E* and *F*) Representative Western blot images for siRNA KDs of TRIM28 and TRIM24 in UMG12 and UWG6 cells. GFP-hTERT was detected with anti-GFP antibody. Quantification of band intensity was done by ImageJ software. (*G* and *H*) qRT-PCR for TRIM28 and hTERT mRNA levels after smartpool siRNA-mediated transient KD of TRIM28 for 72 h in bladder cancer cell lines. (*I* and *J*) qRT-PCR for TRIM24 and hTERT mRNA levels after smartpool siRNA-mediated transient KD of TRIM24 for 72 h in bladder cancer cell lines. Also, reference *SI Appendix*, Fig. S6 *A–D*. −124C > T: heterozygous hTERT promoter mutation; WT: no promoter mutation in indicated cell lines. Graphs represent mean ± SEM, $n = 3$ from independent experiments. **P* value < 0.05; ***P* value < 0.01; ****P* value < 0.001.

lines. TRIM28 depletion nullified the effects of TRIM24 depletion on hTERT mRNA levels, suggesting TRIM24 indirectly regulates hTERT by inhibiting TRIM28 activity (Fig. 5*A* and *SI Appendix*, Fig. S7*C*). This was supported by our finding that TRIM28 and TRIM24 coimmunoprecipitate in UMG12 cells (Fig. 5*B*).

TRIM28 acts as a transcription checkpoint, causing promoter-proximal pausing of RNA polymerase II (Pol II). TRIM28 is well reported to be phosphorylated at Serine-473 and -824 (phosphositeplus database), and depletion or phosphorylation of TRIM28 at Serine-824 releases Pol II pausing, thus activating transcription (43). Phosphorylation of TRIM28 at Serine-473 has also been shown to nullify its repressor activity (44, 45). In UMG12 cells, immunoprecipitation and Western blotting showed phosphorylated TRIM28 does not interact with TRIM24 (Fig. 5*B*). This suggests TRIM24 binds TRIM28 to aid in its transcription repressor activity and that TRIM28 phosphorylation prevents this binding, allowing TRIM28 to activate hTERT transcription. To evaluate this further, we performed chromatin immunoprecipitation (ChIP) for TRIM28 and TRIM24 in UMG12 cells and qRT-PCR on the pulled-down DNA fragments for different hTERT promoter regions. We found TRIM28- and TRIM24-associated fragments were enriched for the hTERT promoter region harboring the −124C > T mutation compared to other regions on the same promoter (Fig. 5 *C* and *D*). PCR with a forward primer before the −124C > T mutation site and a reverse primer at either the GFP or hTERT gene showed amplification only with GFP reverse primer in ChIP samples (Fig. 5*E*). The presence of mutation in PCR samples with GFP reverse primer was confirmed by Sanger sequencing (*SI Appendix*, Fig. S7*D*).

We also mined the Cistrome database (dbtoolkit.cistrome.org/) to look for factors regulating hTERT within 1-kb region to transcription start site (TSS). Since most data are from lines with the WT hTERT promoter, the regulatory potential (RP) score of TRIM28 and TRIM24 for hTERT was low (Fig. 5*F*). This analysis independently suggests that TRIM28 and TRIM24 have lower affinity for the WT hTERT promoter and that TRIM28 and TRIM24 interact and preferentially get recruited to the mutated hTERT promoter.

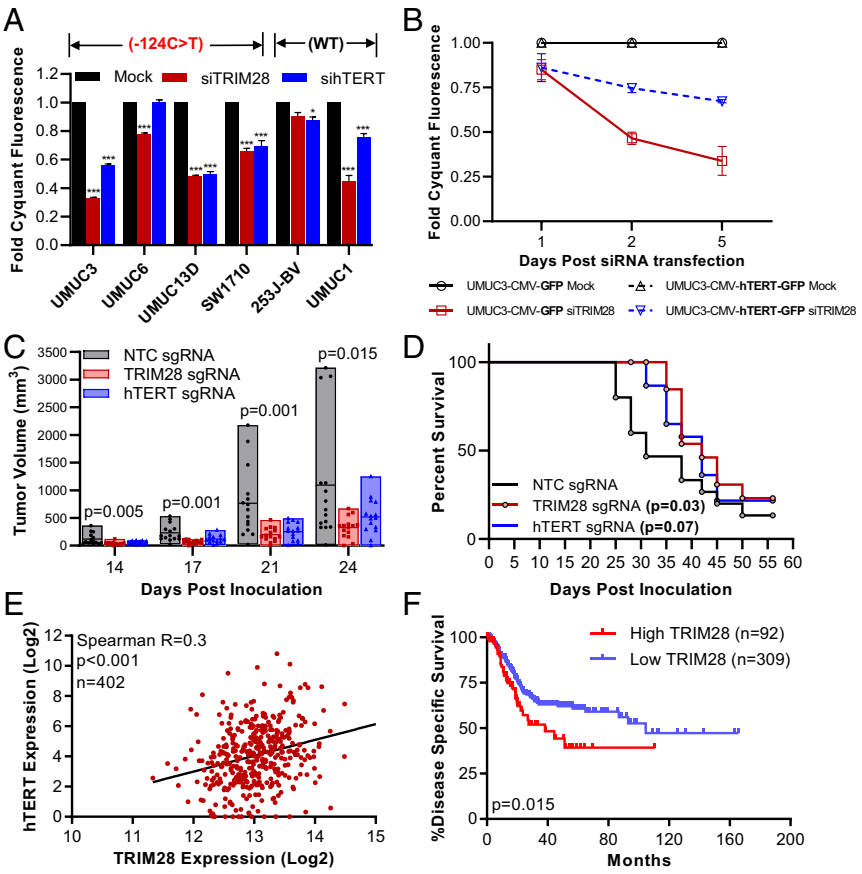

Fig. 4. Biological and clinical relevance of TRIM28 and correlation with hTERT. (*A*) Effect of transient KD of TRIM28 and hTERT on in vitro monolayer growth of different cell lines. −124C > T: heterozygous hTERT promoter mutation; WT: no promoter mutation in indicated cell lines. Bars represent mean ± SEM, $n = 3$ from independent experiments. **P* value < 0.05; ****P* value < 0.001. (*B*) UMUC3 cells overexpressing CMV promoter–driven GFP (UMUC3-CMV-GFP) or hTERT-GFP (UMUC3-CMV-hTERT-GFP) were transiently knocked down with TRIM28 siRNA, and cell growth was monitored over 5 d post-transfection. Mock-treated cells were used as control. (*C*) In vivo subcutaneous tumor growth of UMUC3 cells transduced with lentivirus for either NTC, TRIM28, or hTERT sgRNAs. Box plot showing range as box and mean as line inside the box. $n = 15$ for each group. One-way ANOVA test was used to compare three groups and generate *P* values. (*D*) Survival curve of mice from *C*. Tumors reaching the limit as per IACUC guidelines were used as a cause of death. Gehan–Breslow–Wilcoxon test was used for comparison. (*E*) Correlation between hTERT and TRIM28 mRNA expression from bladder cancer TCGA patient datasets. Negative fold values were converted to 0. Also, reference *SI Appendix*, Fig. S6 *J* and *K*. (*F*) Kaplan–Meier curves for disease-specific survival of bladder cancer patients with high and low TRIM28 expression analyzed from TCGA datasets. Also, reference *SI Appendix*, Fig. S6*L*.

GABPA is a known ETS transcription factor family member, which, along with GABPB1, specifically binds to the hTERT promoter mutation site. To ask if TRIM28 and TRIM24 binding is dependent on GABPA, we depleted it in UMG12 cells using siRNAs and performed ChIP with TRIM28 and TRIM24 antibodies. Knocking down GABPA reduced the binding of both TRIM28 and TRIM24 to the mutated site (Fig. 5*G*). Mutant promoter binding of TRIM24 is dependent on TRIM28, as depleting TRIM28 reduces the binding of TRIM24 along with TRIM28 to the mutant promoter region (Fig. 5*G*). Furthermore, both GABPA and GABPB1 coimmunoprecipitated with TRIM28 but not TRIM24 (Fig. 5*H*). These results suggest that the GABPA-GABPB1 complex recruits TRIM28-TRIM24 to mutant hTERT promoter sites via interaction with TRIM28.

mTOR Phosphorylates TRIM28 to Induce hTERT Transcription. Next, we directed our attention to other kinases that were significantly enriched or depleted with FDR < 0.001 at day 4 in GFP^{Low} or GFP^{High} cells, respectively. These include mTOR, MAP2K3, PRKACA, MAPK14 (p38MAPK), NADK2, and PRKAA1 (Fig. 2*C*). Transiently depleting their mRNAs in UMG12 cells showed that only mTOR and p38MAPK depletion significantly decreased hTERT mRNA expression (Fig. 6*A*). Although the MAPK pathway was previously reported to regulate hTERT (46, 47), mTOR has no known association with hTERT. To understand if they transcriptionally regulate hTERT via the WT or mutant allele, we cultured UMG12 and UWG6 cells as three-dimensional (3D) organoids, which are considered a better physiological model for drug screening than monolayer culture (48). Cells in 3D were treated with specific inhibitors Ridaforolimus (mTOR inhibitor) and Doramapimod (p38MAPK inhibitor), and GFP intensity was monitored using the Opera Phenix High-Content Screening System. We also included UMUC3 cells expressing CMV promoter–driven hTERT-GFP for a negative control. Ridaforolimus reduced GFP intensity more effectively in UMG12 cells (Fig. 6*B* and *SI Appendix*, Fig. S7*E*), while Doramapimod inhibited GFP at similar levels in all three cell lines (Fig. 6*C*). This suggests mTOR specifically regulates hTERT expression from the mutant promoter allele. We confirmed this by treating different cell lines with Ridaforolimus. Cell lines harboring the −124C > T mutation showed decreased hTERT mRNA expression, whereas there was no expression change in 253J-BV cells (Fig. 6*D*).

Since mTOR has been reported to phosphorylate TRIM28 at Ser-824 to suppress its transcriptional repressor activity (49), we hypothesized that mTOR might regulate hTERT through

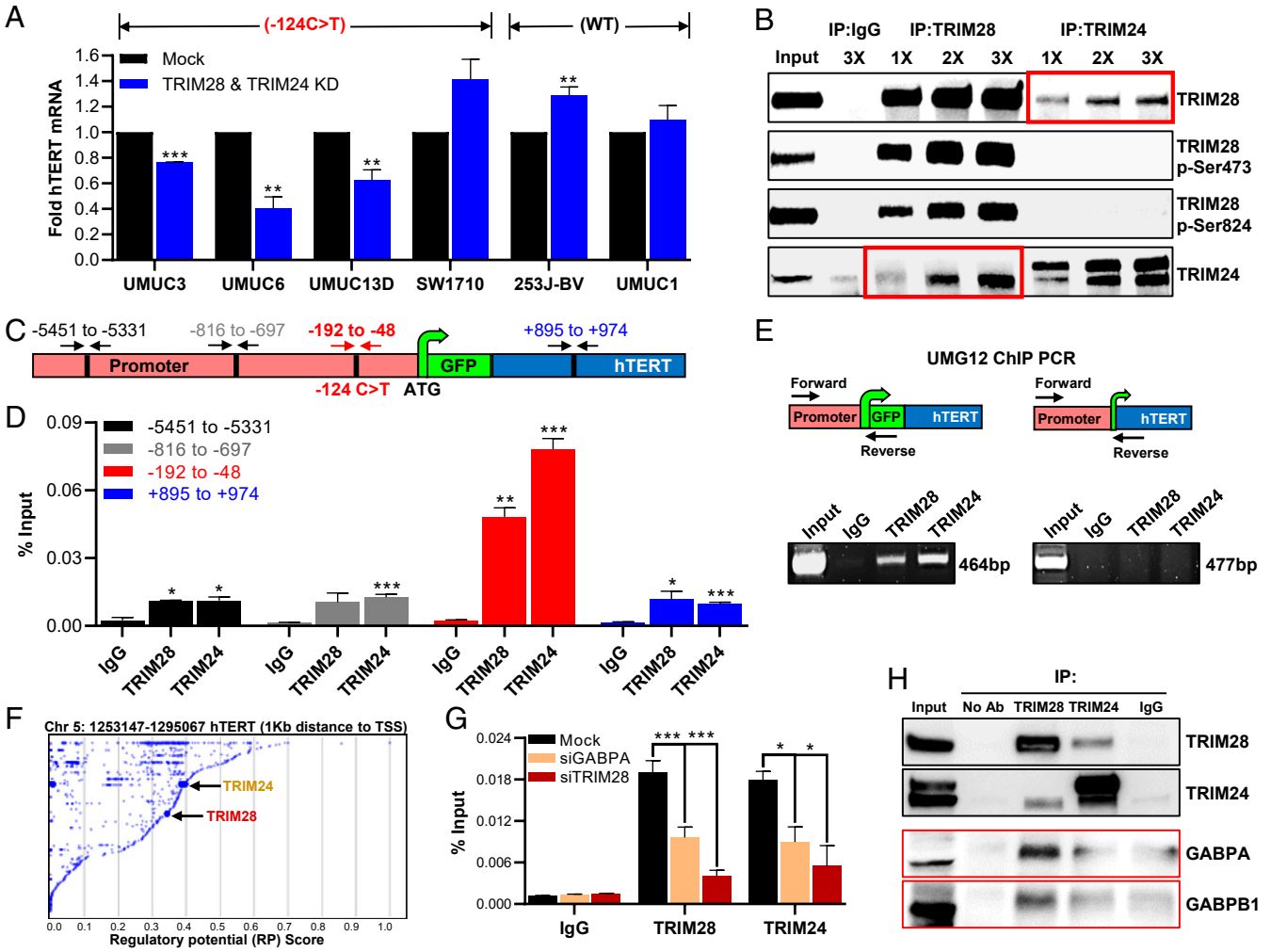

Fig. 5. TRIM28 and TRIM24 interact and bind to mutant hTERT promoter region. (*A*) hTERT mRNA after double KD of TRIM28 and TRIM24 with siRNAs for 72 h. −124C > T: heterozygous hTERT promoter mutation; WT: no promoter mutation in indicated cell lines. (*B*) Endogenous coimmunoprecipitation (Co-IP) in UMG12 cells. Whole-cell lysates at three dilutions were incubated with TRIM28 or TRIM24 antibodies for IP. IgG antibody used as control. Coimmunoprecipitated bands are in the red box. (*C*) Schematic diagram of hTERT allele showing primer positions used for ChIP qRT-PCR. (*D*) TRIM28, TRIM24, or IgG control ChIP qRT-PCR for hTERT allele in UMG12 cells. *P* values were derived from differences between IgG and TRIM28 or TRIM24. (*E*) PCR amplification of ChIP samples as indicated. (*F*) Plot generated from Cistrome database showing regulatory potential of TRIM28 and TRIM24 for hTERT. (*G*) ChIP qRT-PCR with IgG, TRIM28, and TRIM24 antibodies in UMG12 cells transiently knocked down with GABPA and TRIM28 siRNAs for 72 h. Bars represent enrichment for hTERT mutant promoter region (−192 to −48). Graphs represent mean ± SEM, $n = 3$ from independent experiments. **P* value < 0.05; ***P* value < 0.01; ****P* value < 0.001. (*H*) Endogenous Co-IP in UMG12 cells using indicated antibodies.

TRIM28 phosphorylation. To test this, we knocked down mTOR in UMG12 cells and found reduced phosphorylation of TRIM28 at both Serine-473 and -824 along with reduced GFP-hTERT protein levels. Total TRIM28 protein levels were unaffected by mTOR KD (Fig. 6*E*). mTOR acts as a catalytic subunit of two structurally different complexes, mTOR complex 1 (mTORC1) and mTORC2. We treated UMG12 cells with Ridaforolimus and JR-AB2-011, which are reported to be specific inhibitors for mTORC1 (50) and mTORC2 (51), respectively. This was further confirmed in our model system, as JR-AB2-011 did not affect phosphorylation of mTOR at Serine 2448, which is specifically phosphorylated by the mTORC1 complex (52). We found only Ridaforolimus suppressed TRIM28 phosphorylation and GFP-hTERT expression (Fig. 6*F*). Furthermore, we observed that Ridaforolimus treatment reduces the binding of TRIM28 and TRIM24 to the mutant promoter site in UMG12 cells (Fig. 6*G*).

To confirm the role of phosphorylated TRIM28 in activating hTERT transcription, we created phospho-mimetic and phospho-dead TRIM28 mutant plasmids by replacing serines at 473 and 824 amino acid positions with either glutamic acid or alanine and transfected in UMG12 cells along with the WT TRIM28 plasmid. GFP-hTERT protein levels were increased in cells overexpressing WT TRIM28 compared to empty vector control. The phospho-mimetic TRIM28 has more up-regulation of GFP-hTERT compared to WT or phospho-dead TRIM28 after correcting for their overexpression levels (Fig. 6*H*). Furthermore, viability assays in UMG12 cells found cell growth defects in monolayer and soft agar resulting from mTOR KD and were amplified by Ridaforolimus (Fig. 6 *I* and *J*).

Based on the observed opposing effects of TRIM28 and TRIM24 on hTERT, we sought to ask if this is specific to hTERT regulation or also true in general. We performed RNA sequencing (RNA-seq) by individually knocking down hTERT, TRIM28, TRIM24, and mTOR in UMG12 cells. The KD of each gene was confirmed both by qRT-PCR (*SI Appendix*, Fig. S8*A*) and by comparing read counts from RNA-seq data (*SI Appendix*, Fig. S8*B*). First, we checked the effect of TRIM28, mTOR, and TRIM24 KD on hTERT and GFP transcripts and found

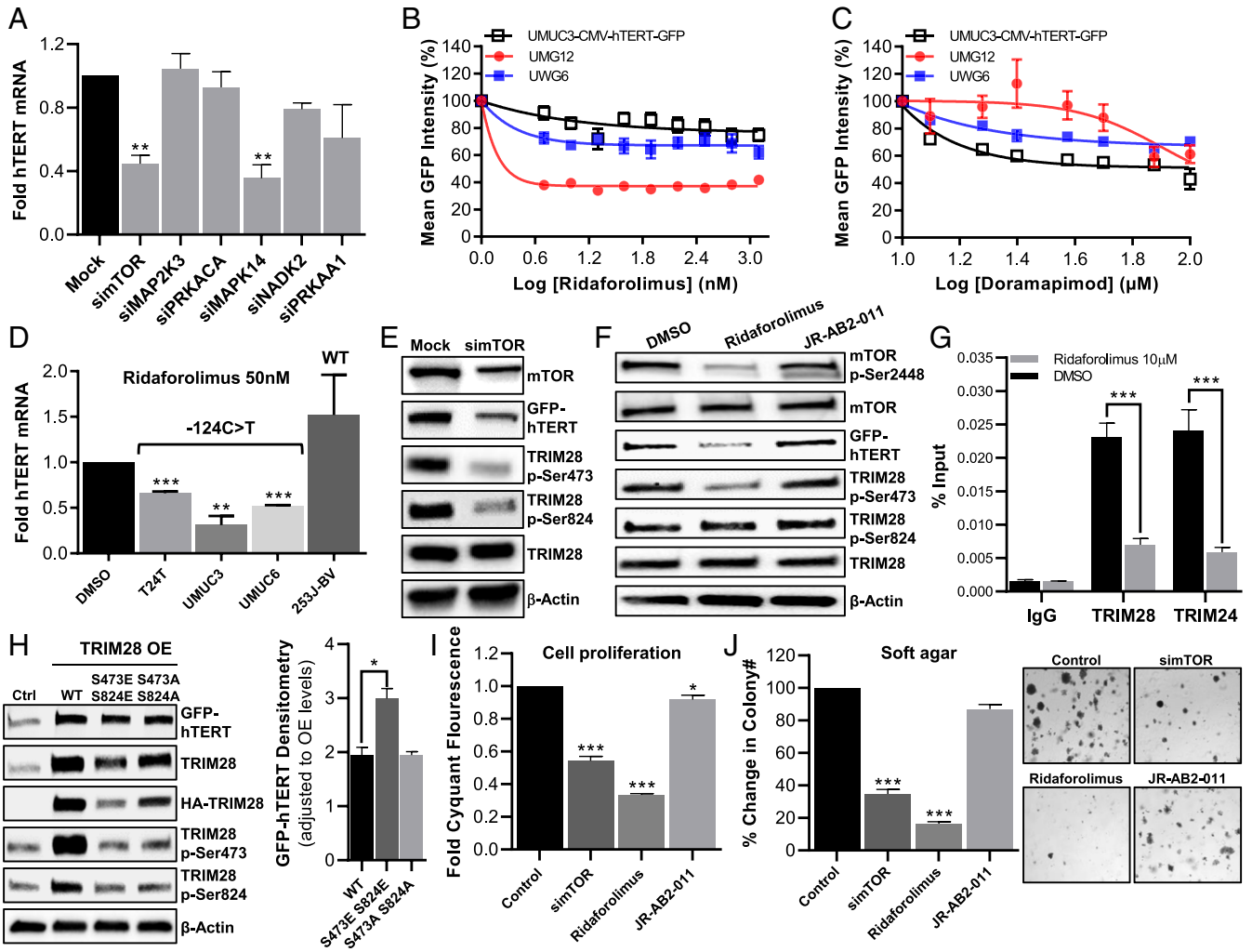

Fig. 6. mTOR mediates TRIM28 phosphorylation to induce hTERT reactivation from mutant promoter. (*A*) hTERT mRNA after depletion of other screen hits in UMG12 cells. 3D-cultured cells treated with (*B*) Ridaforolimus and (*C*) Doramapimod for 72 h. Also reference *SI Appendix*, Fig. S7*E*. (*D*) 3D-cultured cells treated with Ridaforolimus at 50 nM concentration, and hTERT mRNA measured after 72 h. −124C > T: heterozygous hTERT promoter mutation; WT: no promoter mutation in indicated cell lines. (*E*) Western blot images of UMG12 cells depleted of mTOR. (*F*) UMG12 treated with 10 μM drugs. Dimethyl sulfoxide (DMSO) used as control. (*G*) UMG12 cells treated with DMSO or Ridaforolimus for 72 hr were processed for ChIP qRT-PCR with IgG, TRIM28, and TRIM24. Bars represents enrichment for hTERT mutant promoter region (−192 to −48). (*H*) Western blot images for UMG12 cells overexpressed with TRIM28 plasmids for 96 hr. WT: no mutation, S473E S824E: Serine to Glutamic acid at 473 and 824 amino acids; S473A S824A: Serine to Alanine at 473 and 824 amino acids. UMG12 with simTOR or drug treated at 10 μM were processed for (*I*) cell proliferation assay and (*J*) soft agar assay. (*Right*) Representative images of soft agar colonies. Graphs represent mean ± SEM, $n = 3$ from independent experiments. *P value < 0.05; **P value < 0.01; ***P value < 0.001.

agreement with our prior findings (Fig. 7*A*). t-distributed stochastic neighbor embedding analysis of all the samples with significantly altered genes showed that hTERT, TRIM28, and mTOR KD samples clustered close to each other, while TRIM24 KD samples clustered distantly (*SI Appendix*, Fig. S8*C*). This clearly indicates that hTERT, TRIM28, and mTOR are in the same pathway, while TRIM24 is a repressor of this pathway. Furthermore, hierarchical clustering of genes with significant differential expression clearly showed that TRIM28 and TRIM24 have opposing roles in terms of regulating genes in general (Fig. 7*B*). An ingenuity pathway analysis (IPA)-based analysis of the pathways related to these genes found that knocking down of any of TRIM28, mTOR, or hTERT caused cell proliferation and cell cycle pathways to be silenced and cell death pathways to be activated (Fig. 7*C*). These data were consistent with our experimental in vitro (Fig. 4*A* and *SI Appendix*, Fig. S6*F*) and in vivo biological data (Fig. 4 *C* and *D*) and with clinical findings in patients (Fig. 4*F* and *SI Appendix*, Fig. S6*L*).

Discussion

Monitoring hTERT expression from endogenous mutant promoters is challenging, as most cancer cell lines have a heterozygous mutation. We addressed this successfully by generating clonal cell lines from the UMUC3 human bladder cancer cell line, which harbors a heterozygous −124C > T promoter mutation, with the insertion of an enhanced GFP tag at either a WT or −124C > T mutant promoter allele. As endogenous hTERT expression is very weak, we used enhanced GFP, which has 35-fold brighter intensity and is more stable than WT GFP (53), to be able to detect signal from the GFP-hTERT fusion protein by microscopy and flow cytometry. We observed higher GFP-hTERT expression from the mutant promoter allele compared to the WT allele. This is consistent with the mutant hTERT promoter being more active as reported previously (8, 14), although we cannot rule out differences in number of copies of respective alleles tagged with GFP in each clone. We confirmed the correct integration of GFP as we detected the full-length

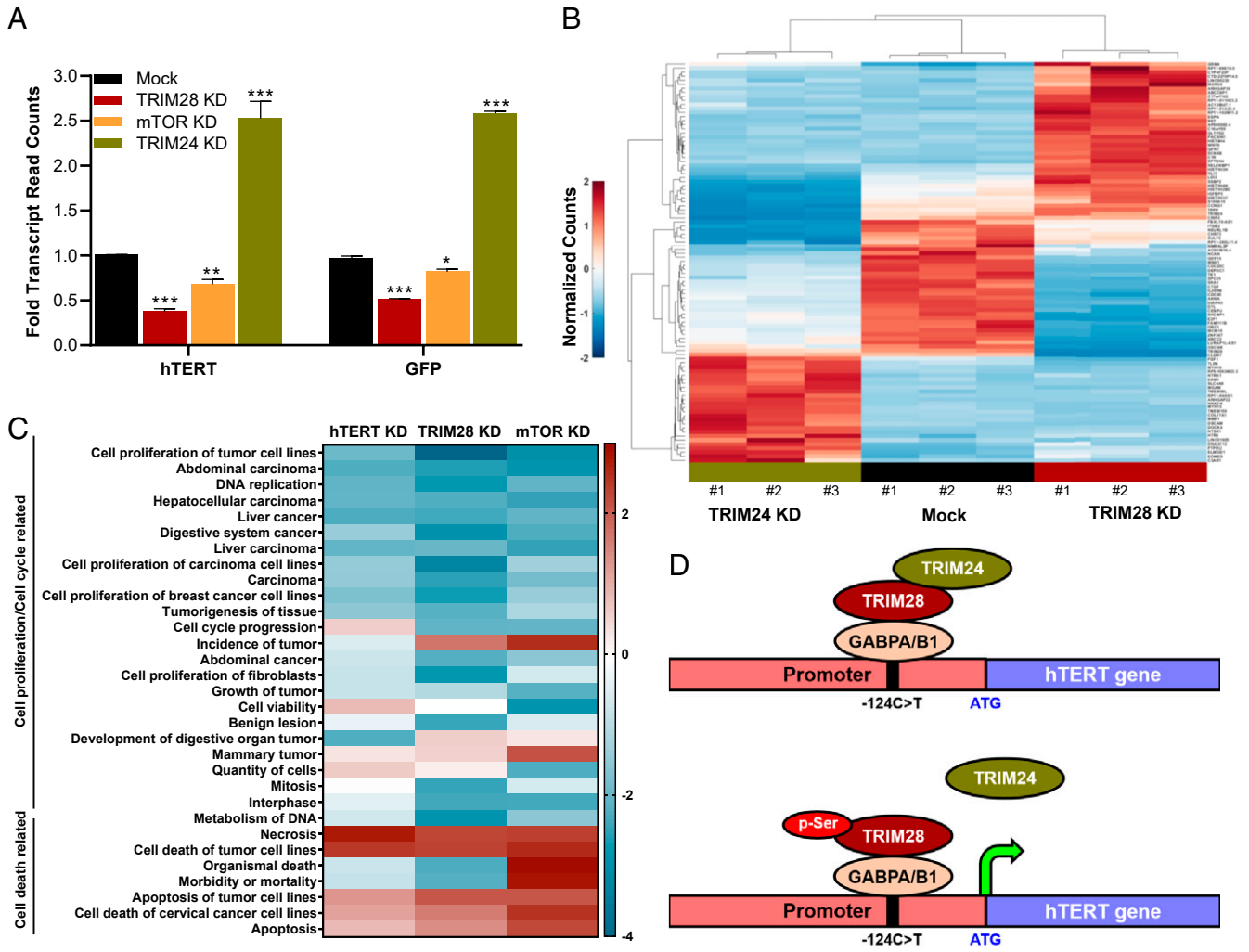

Fig. 7. RNA-seq analysis supports the signaling pathway involving hTERT, TRIM28, TRIM24, and mTOR. (*A*) Levels of hTERT and GFP transcripts from RNA-seq data with KD of indicated genes in UMG12 cells. **P* value < 0.05; ***P* value < 0.01; ****P* value < 0.001. (*B*) Hierarchical clustering of 25 most up-regulated and 25 most down-regulated genes in each replicate of Mock, TRIM28 KD, and TRIM24 KD UMG12 cells. (*C*) Heat map of diseases and biofunctions pathways altered in all three comparisons with *Z*-score more than ±2 in at least one comparison. (*D*) Model diagram of proposed mechanism for regulation of hTERT reactivation from mutant hTERT promoter.

GFP-hTERT protein whose expression decreased with hTERT siRNA. This was further confirmed at the mRNA level by a decrease in hTERT mRNA following the KD of GFP and GABPA.

A functional Kinome KO screen in the UMG12 clone tagged with GFP at the mutant hTERT promoter allele revealed TRIM28 as an activator and TRIM24 as a repressor of hTERT expression from the mutant promoter. TRIM28 is involved in the regulation of gene transcription, response to DNA damage, down-regulation of p53 activity, stimulation of EMT, stemness sustainability, induction of autophagy, and regulation of retrotransposition (42). TRIM24, a coregulator of transcription, can act as an oncogene or tumor suppressor in a context-dependent manner (54). TRIM28 may be a good therapeutic target as, even though it is ubiquitously expressed in most of the body organs (https://www.gtexportal.org) and is embryonic lethal in mice, its depletion in adult mice is not associated with any behavioral or pathological changes (55).

Expression of TRIM28 tracks with hTERT expression in bladder cancer, melanoma, and glioblastoma cancer types, which possess the highest frequency of hTERT promoter mutations. However, there are cases in which TRIM28 and hTERT do not have a positive correlation, suggesting that other factors may also be regulating hTERT expression. Also, since we do not yet have enough information to stratify patient samples based on both hTERT promoter mutation and expression, it is possible that samples with negative or zero correlation do not have the promoter mutation. Like hTERT, higher TRIM28 is also associated with worse disease-specific survival. However, positive correlation between TRIM28 and worse prognosis could be due to its effect on expression of genes other than hTERT. Our in vitro cell growth experiments also showed that depleting TRIM28 or hTERT reduces short-term cell growth. We observed a similar trend in the growth rates of tumors generated with UMUC3 cells knocked down for TRIM28 and hTERT. The effect of hTERT inhibition on short-term cell growth in cancer cell lines supports the notion that hTERT has noncanonical functions because telomere-specific functions normally require many population doublings before they are revealed. This is also supported by our RNA-seq data in which short-term KD of hTERT caused down-regulation of cell proliferation and cell cycle–related genes with an up-regulation of cell death–related genes. TRIM28 depletion in bladder cancer, glioblastoma, and melanoma cell lines suppressed cell growth. Its depletion significantly reduced tumor

growth in mice and increased survival. Our rescue experiment suggested that the effect of TRIM28 on cancer cell growth is in part mediated by activating hTERT transcription and potentially involves other mechanisms as well. High TRIM28 expression is associated with worse disease-specific survival in bladder cancer and melanoma. These findings position TRIM28 as a therapeutically tractable positive regulator of mutant promoter–driven hTERT expression.

Phosphorylation of TRIM28 at Serine-473 and -824 is known to induce its transcriptional activator activity. TRIM28 causes pausing of RNA Pol II at the transcription start site, while its phosphorylation at Ser-824 releases that pause (43). Phosphorylation of TRIM28 at Ser-473 is also involved in efficient DNA repair, cell survival upon DNA damage, and a molecular switch for the regulation of gene expression (44, 56, 57). Our ChIP studies determined that TRIM28 and TRIM24 are recruited to the −124C > T mutated promoter region through GABPA. However, phosphorylation of TRIM28 is required to activate hTERT transcription by disrupting its interaction with TRIM24. GABPA/B1 interacts with TRIM28 to facilitate its recruitment at the mutant promoter site. TRIM33 was also identified as a hit in the CRISPR screen and, interestingly, among more than 70 known TRIM family members, only TRIM28, TRIM24, and TRIM33 possess the PHD and Bromo domains, which are involved in chromatin remodeling (58). It may be worth investigating further if and how TRIM33 is involved in TRIM28- and TRIM24-mediated regulation of hTERT.

mTOR and MAPK pathway genes were also identified as mutant promoter activators. Though the MAPK pathway was previously linked with hTERT expression, mTOR had not been associated with hTERT transcriptional regulation. Our results with kinase inhibitors suggest that the MAPK pathway is not specific to the mutant promoters in the UMUC3 cell line since we observed a similar level of inhibition in UMG12 and UWG6 cells. Furthermore, MAPK inhibitor also decreased hTERT levels in UMUC3 cells with CMV promoter-driven hTERT-GFP (Fig. 6*C*). The mTOR inhibitor Ridaforolimus is specific to mutant promoter regulation since it decreased GFP intensity in UMG12 cells more effectively than in UWG6 or UMUC3-CMV-hTERT-GFP cells. mTOR signaling mainly regulates cell proliferation and metabolism involved in tumor initiation and progression. It is enhanced in various cancer types with almost 30% of solid tumors showing dysregulation (59). mTOR is the second most frequently altered pathway after p53 in human cancers (60). In our model system, mTOR KD or inhibition prevented TRIM28 phosphorylation and suppressed hTERT expression, which we traced to the mTORC1 complex. Only mTORC1 inhibition with Ridaforolimus blocked hTERT and TRIM28 phosphorylation. Ridaforolimus also reduced the binding of TRIM28 and TRIM24 to the hTERT promoter mutation site. This suggests that the mTORC1 pathway promotes hTERT expression from the mutant promoter by phosphorylating TRIM28, releasing it as an activator from the repressor TRIM24 to promote transcription. The clinical relevance of these findings is supported by data showing reciprocal prognostication of various components in this pathway coupled with unbiased differential gene expression analysis, suggesting hTERT inhibition is similar to TRIM28 and mTOR inhibition in terms of which genes are dysregulated. It would be interesting to explore what pathways or factors trigger mTOR-mediated phosphorylation of TRIM28 leading to hTERT transcriptional activation. Inhibiting mTORC1 with Ridaforolimus also suppressed bladder cancer cell growth. Since we did not see complete inhibition of cell growth with TRIM28 depletion or mTOR inhibition, this suggests future combination therapies will be needed to achieve complete tumor eradication.

In conclusion, our findings support the putative mechanism that the TRIM28-TRIM24 complex is recruited to the hTERT promoter mutation site through the GABPA/B1 complex and that the phosphorylation of TRIM28 is required to activate hTERT transcription by releasing TRIM24 from the mutation site (Fig. 7*D*). Using a platform to monitor the allele-specific expression of hTERT within cancer cell lines, we discovered a signaling pathway regulating hTERT expression from the mutant promoter that may represent an effective precision therapeutic strategy for cancer patients with hTERT promoter mutations. mTORC1-specific inhibitors target this pathway and may therefore be of therapeutic benefit for cancer patients with hTERT promoter mutations and hTERT overexpression.

Materials and Methods

Generation of hTERT KO Clones. UMG12 cells were transduced with lentivirus containing hTERT sgRNA ligated to Cas9 plasmid pXPR-206. After selecting with puromycin, cells were seeded in 96-well plates at one cell/well. Single-cell clones were expanded and screened for hTERT KO by Western blotting with GFP antibody. Clones with undetectable GFP-hTERT band at 160 KD were considered as hTERT KO.

CRISPR Pooled Screen Readout and Data Analysis. Sequencing files were demultiplexed by Novogene and analyzed at Cedars-Sinai Medical Center, Los Angeles. For quality control assessment of sequencing results, MAGeCK-VISPR was used (40). sgRNAs from sorted cells were compared to unsorted cells for enrichment at both time points using a robust MAGeCK algorithm (41). Briefly, MAGeCK-VISPR is designed for quality control (QC) and analyzing CRISPR screening results. First, it does the QC analysis at four levels: sequence, read count, sample, and gene. After QC, the MAGeCK-MLE (maximum likelihood estimation) algorithm gives the significantly altered genes between two conditions. For a detailed description of MAGeCK-VISPR, see Li et al. (40).

Kinase Inhibitor Treatment in 3D Tumor Organoid Assays. Ridaforolimus and Doramapimod were purchased from SelleckChem. UMG12, UWG6, and UMUC3-CMV-hTERT-GFP cells were used for treatment with kinase inhibitors. Uniform single cells were plated at a density of 10,000 cells/well in round bottom ultra-low attachment 96-well plates (PerkinElmer). After centrifugation at 1,000 rpm for 15 min for cell aggregation, cells were incubated for 3 d with 2% of growth factor–reduced Matrigel (Corning) in phenol red-free media and treated with Ridaforolimus and Doramapimod at various concentrations in triplicates. All organoids had a diameter above 300 μm and were stained with Hoechst 33342 before imaging with the Opera Phenix Imaging System (PerkinElmer). The single organoids were imaged on a 5× air objective (PerkinElmer) recording 15 confocal z-stack images in 20-μm steps and using a total of three channels for brightfield, Hoechst, and GFP. Images were analyzed with the Harmony software 4.9 (PerkinElmer). In brief, organoids were analyzed in the maximum projection configuration. The organoid selection criteria were based on roundness and region area based on the Hoechst channel. Background subtraction was performed by defining the surrounding region. GFP intensity was averaged for all the organoid z-stacks.

Coimmunoprecipitation. For immunoprecipitation (IP), cells were harvested and lysed with IP lysis buffer (Pierce) supplemented with Halt protease and phosphatase inhibitor mixtures (Fisher Scientific). Approximately 200 (1×), 400 (2×), and 600 (3×) μg protein from whole-cell lysate was incubated with antibodies conjugated to Protein G Sepharose 4 Fast Flow Beads (GE Healthcare) at 4 °C overnight. Antibodies used for IP are listed in *SI Appendix*, Table 2. A matched isotype antibody was used as a negative control. After washing 4× with lysis buffer, precipitated protein complexes were extracted with 1× Laemmli sodium dodecyl sulfate (SDS) sample buffer and processed for Western blotting.

Fluorescence-Activated Cell Sorting Analysis and Sorting. For fluorescence-activated cell sorting (FACS) analysis, cells were suspended in 1% bovine serum albumin in 1× Dulbecco's phosphate-buffered saline (PBS) and analyzed for GFP signal, and DAPI was used as a live/dead cell marker. FACS analysis was done using CyAN or BD LSCII flow cytometer. For FACS sorting, cells were detached with PBS-ethylenediaminetetraacetic acid (EDTA) and suspended in phenol red-free minimal essential medium with 2% fetal bovine serum and kept at room temperature. Sorting was done using a Moflo XDP100 flow sorter. Sorting for library screening was done at a high speed of ~20,000 events/second using Moflo XDP70 flow sorter to reduce the time of cells in the sorting buffer. All flow sorting was done at the Flow Cytometry Core at the University of Colorado Cancer Center, while additional FACS analysis was also done at the Flow Cytometry Core at Cedars-Sinai Medical Center (CSMC).

Telomere Length by Southern Blotting. TRF length analysis was carried out as described (61). Briefly, genomic DNA (gDNA) was isolated from cells using Quick-DNA Miniprep Kit (11-317AC; Zymo Research). A total of 1.5 to 4.5 μg gDNA from each cell line was digested with RsaI and HinfI. Digested gDNA samples were resolved on a 0.8% agarose gel. The DNA was then transferred to Hybond N+ nylon membrane (GE), which was probed for a telomeric sequence using a radiolabeled $(TTAGGG)^4$ probe. The membrane was imaged using phosphor screens and a Typhoon FLA 9500 Imager (GE). To calculate mean telomere length, lane intensity profiles were extracted using ImageJ, median points were found using Microsoft Excel, and the DNA lengths corresponding to these points were calculated using a λ-HindIII molecular weight marker (New England Biolabs).

DNA FISH Analysis. DNA fluorescence in situ hybridization (FISH) using hTERT-specific probes (Empire Genomics; TERT-20-OR) for UMUC3 and its subclones were performed by the WiCell Research Institute Characterization Laboratory. Cells were cultured in T25 flasks as per the requirements and shipped to WiCell for further processing.

Study Approval. Mouse studies conducted were approved by Institutional Animal Care and Use Committee and in strict accordance with CSMC animal ethics guidelines.

Data Availability. RNA-seq data have been deposited in the Gene Expression Omnibus (GSE181461). All other study data are included in the article and/or supporting information.

ACKNOWLEDGMENTS. We thank Jinfen Xiao, Esra Ibili, and Megan M. Tu for technical help and the D.T. and T.R.C. laboratories for fruitful discussions. We thank Guarnerio Laboratory at CSMC for providing extra resources. We also thank the University of Colorado Skaggs School of Pharmacy High Throughput Screening Drug Discovery and Chemical Biology Core Facility for their contribution to this work. The HTS Core has been supported in part by the State of Colorado Office of Economic Development and the Colorado Clinical and Translational Sciences Institute (NIH Grant UL1TR001082), The University of Colorado Anschutz Medical Campus. S.R. was supported by the Cancer Foundation of Luxembourg. This work was supported by Department of Defense Congressionally Directed Medical Research Program CA180175 to D.T. T.R.C. is an investigator of the HHMI.

1. D. Hanahan, R. A. Weinberg, Hallmarks of cancer: The next generation. *Cell* **144**, 646–674 (2011).
2. A. J. Colebatch, A. Dobrovic, W. A. Cooper, *TERT* gene: Its function and dysregulation in cancer. *J. Clin. Pathol.* **72**, 281–284 (2019).
3. S. C. Akincilar, B. Unal, V. Tergaonkar, Reactivation of telomerase in cancer. *Cell. Mol. Life Sci.* **73**, 1659–1670 (2016).
4. R. Hrdlicková, J. Nehyba, H. R. Bose Jr, Alternatively spliced telomerase reverse transcriptase variants lacking telomerase activity stimulate cell proliferation. *Mol. Cell. Biol.* **32**, 4283–4296 (2012).
5. I. Listerman, J. Sun, F. S. Gazzaniga, J. L. Lukas, E. H. Blackburn, The major reverse transcriptase-incompetent splice variant of the human telomerase protein inhibits telomerase activity but protects from apoptosis. *Cancer Res.* **73**, 2817–2828 (2013).
6. L. L. Smith, H. A. Coller, J. M. Roberts, Telomerase modulates expression of growth-controlling genes and enhances cell proliferation. *Nat. Cell Biol.* **5**, 474–479 (2003).
7. S. Mukherjee, E. J. Firpo, Y. Wang, J. M. Roberts, Separation of telomerase functions by reverse genetics. *Proc. Natl. Acad. Sci. U.S.A.* **108**, E1363–E1371 (2011).
8. S. Borah *et al.*, Cancer. TERT promoter mutations and telomerase reactivation in urothelial cancer. *Science* **347**, 1006–1010 (2015).
9. T. Liu, X. Yuan, D. Xu, Cancer-specific telomerase reverse transcriptase (TERT) promoter mutations: Biological and clinical implications. *Genes (Basel)* **7**, 38 (2016).
10. F. P. Barthel *et al.*, Systematic analysis of telomere length and somatic alterations in 31 cancer types. *Nat. Genet.* **49**, 349–357 (2017).
11. R. Ma *et al.*, The TERT locus genotypes of rs2736100-CC/CA and rs2736098-AA predict shorter survival in renal cell carcinoma. *Urol Oncol* **37**, 301 e301–301 e310 (2019).
12. A. Zehir *et al.*, Mutational landscape of metastatic cancer revealed from prospective clinical sequencing of 10,000 patients. *Nat. Med.* **23**, 703–713 (2017).
13. S. Horn *et al.*, *TERT* promoter mutations in familial and sporadic melanoma. *Science* **339**, 959–961 (2013).
14. F. W. Huang *et al.*, Highly recurrent *TERT* promoter mutations in human melanoma. *Science* **339**, 957–959 (2013).
15. F. Sahm *et al.*, TERT promoter mutations and risk of recurrence in meningioma. *J. Natl. Cancer Inst.* **108**, djv377 (2015).
16. X. Wang *et al.*, Association of telomerase reverse transcriptase promoter mutations with the prognosis of glioma patients: A meta-analysis. *Mol. Neurobiol.* **53**, 2726–2732 (2016).
17. P. S. Rachakonda *et al.*, TERT promoter mutations in bladder cancer affect patient survival and disease recurrence through modification by a common polymorphism. *Proc. Natl. Acad. Sci. U.S.A.* **110**, 17426–17431 (2013).
18. M. Peifer *et al.*, Telomerase activation by genomic rearrangements in high-risk neuroblastoma. *Nature* **526**, 700–704 (2015).
19. E. T. Sugarman, G. Zhang, J. W. Shay, In perspective: An update on telomere targeting in cancer. *Mol. Carcinog.* **58**, 1581–1588 (2019).
20. M. Ruden, N. Puri, Novel anticancer therapeutics targeting telomerase. *Cancer Treat. Rev.* **39**, 444–456 (2013).
21. A. A. Chiappori *et al.*, A randomized phase II study of the telomerase inhibitor imetelstat as maintenance therapy for advanced non-small-cell lung cancer. *Ann. Oncol.* **26**, 354–362 (2015).
22. R. Salloum *et al.*, A molecular biology and phase II study of imetelstat (GRN163L) in children with recurrent or refractory central nervous system malignancies: A pediatric brain tumor consortium study. *J. Neurooncol.* **129**, 443–451 (2016).
23. R. E. Frink *et al.*, Telomerase inhibitor imetelstat has preclinical activity across the spectrum of non-small cell lung cancer oncogenotypes in a telomere length dependent manner. *Oncotarget* **7**, 31639–31651 (2016).
24. K. J. Wu *et al.*, Direct activation of TERT transcription by c-MYC. *Nat. Genet.* **21**, 220–224 (1999).
25. L. Yin, A. K. Hubbard, C. Giardina, NF-kappa B regulates transcription of the mouse telomerase catalytic subunit. *J. Biol. Chem.* **275**, 36671–36675 (2000).
26. Y. Zhang, L. Toh, P. Lau, X. Wang, Human telomerase reverse transcriptase (hTERT) is a novel target of the Wnt/β-catenin pathway in human cancer. *J. Biol. Chem.* **287**, 32494–32511 (2012).
27. R. J. Bell *et al.*, The transcription factor GABP selectively binds and activates the mutant TERT promoter in cancer. *Science* **348**, 1036–1039 (2015).
28. J. L. Stern, D. Theodorescu, B. Vogelstein, N. Papadopoulos, T. R. Cech, Mutation of the TERT promoter, switch to active chromatin, and monoallelic TERT expression in multiple cancers. *Genes Dev.* **29**, 2219–2224 (2015).
29. S. C. Akıncılar *et al.*, Long-range chromatin interactions drive mutant TERT promoter activation. *Cancer Discov.* **6**, 1276–1291 (2016).
30. A. Mancini *et al.*, Disruption of the β1L isoform of GABP reverses glioblastoma replicative immortality in a TERT promoter mutation-dependent manner. *Cancer Cell* **34**, 513–528.e8 (2018).
31. X. Yuan, C. Larsson, D. Xu, Mechanisms underlying the activation of TERT transcription and telomerase activity in human cancer: Old actors and new players. *Oncogene* **38**, 6172–6183 (2019).
32. Y. Guo *et al.*, GABPA is a master regulator of luminal identity and restrains aggressive diseases in bladder cancer. *Cell Death Differ.* **27**, 1862–1877 (2020).
33. X. Yuan, M. Dai, D. Xu, TERT promoter mutations and GABP transcription factors in carcinogenesis: More foes than friends. *Cancer Lett.* **493**, 1–9 (2020).
34. T. Horbach, C. Götz, T. Kietzmann, E. Y. Dimova, Protein kinases as switches for the function of upstream stimulatory factors: Implications for tissue injury and cancer. *Front. Pharmacol.* **6**, 3 (2015).
35. T. Hunter, M. Karin, The regulation of transcription by phosphorylation. *Cell* **70**, 375–387 (1992).
36. I. Kinde *et al.*, TERT promoter mutations occur early in urothelial neoplasia and are biomarkers of early disease and disease recurrence in urine. *Cancer Res.* **73**, 7162–7167 (2013).
37. J. Lin *et al.*, Nucleolar localization of TERT is unrelated to telomerase function in human cells. *J. Cell Sci.* **121**, 2169–2176 (2008).
38. J. C. Schmidt, A. J. Zaug, T. R. Cech, Live cell imaging reveals the dynamics of telomerase recruitment to telomeres. *Cell* **166**, 1188–1197.e9 (2016).
39. J. G. Doench *et al.*, Optimized sgRNA design to maximize activity and minimize off-target effects of CRISPR-Cas9. *Nat. Biotechnol.* **34**, 184–191 (2016).
40. W. Li *et al.*, Quality control, modeling, and visualization of CRISPR screens with MAGeCK-VISPR. *Genome Biol.* **16**, 281 (2015).
41. W. Li *et al.*, MAGeCK enables robust identification of essential genes from genome-scale CRISPR/Cas9 knockout screens. *Genome Biol.* **15**, 554 (2014).
42. P. Czerwińska, S. Mazurek, M. Wiznerowicz, The complexity of TRIM28 contribution to cancer. *J. Biomed. Sci.* **24**, 63 (2017).
43. H. Bunch *et al.*, TRIM28 regulates RNA polymerase II promoter-proximal pausing and pause release. *Nat. Struct. Mol. Biol.* **21**, 876–883 (2014).
44. C. W. Chang *et al.*, Phosphorylation at Ser473 regulates heterochromatin protein 1 binding and corepressor function of TIF1beta/KAP1. *BMC Mol. Biol.* **9**, 61 (2008).
45. K. Singh *et al.*, A KAP1 phosphorylation switch controls MyoD function during skeletal muscle differentiation. *Genes Dev.* **29**, 513–525 (2015).
46. R. Liu, T. Zhang, G. Zhu, M. Xing, Regulation of mutant TERT by BRAF V600E/MAP kinase pathway through FOS/GABP in human cancer. *Nat. Commun.* **9**, 579 (2018).
47. J. L. Stern *et al.*, Mesenchymal and MAPK expression signatures associate with telomerase promoter mutations in multiple cancers. *Mol. Cancer Res.* **18**, 1050–1062 (2020).
48. F. Mittler *et al.*, High-content monitoring of drug effects in a 3D spheroid model. *Front. Oncol.* **7**, 293 (2017).
49. B. Rauwel *et al.*, Release of human cytomegalovirus from latency by a KAP1/TRIM28 phosphorylation switch. *eLife* **4**, e06068 (2015).
50. E. Vilar, J. Perez-Garcia, J. Tabernero, Pushing the envelope in the mTOR pathway: The second generation of inhibitors. *Mol. Cancer Ther.* **10**, 395–403 (2011).
51. A. Benavides-Serrato *et al.*, Specific blockade of Rictor-mTOR association inhibits mTORC2 activity and is cytotoxic in glioblastoma. *PLoS One* **12**, e0176599 (2017).
52. J. Copp, G. Manning, T. Hunter, TORC-specific phosphorylation of mammalian target of rapamycin (mTOR): Phospho-Ser2481 is a marker for intact mTOR signaling complex 2. *Cancer Res.* **69**, 1821–1827 (2009).
53. X. Li *et al.*, Deletions of the Aequorea victoria green fluorescent protein define the minimal domain required for fluorescence. *J. Biol. Chem.* **272**, 28545–28549 (1997).

54. W. W. Tsai *et al.*, TRIM24 links a non-canonical histone signature to breast cancer. *Nature* **468**, 927–932 (2010).
55. M. W. Rousseaux *et al.*, Depleting Trim28 in adult mice is well tolerated and reduces levels of α-synuclein and tau. *eLife* **7**, e36768 (2018).
56. D. White *et al.*, The ATM substrate KAP1 controls DNA repair in heterochromatin: Regulation by HP1 proteins and serine 473/824 phosphorylation. *Mol. Cancer Res.* **10**, 401–414 (2012).
57. D. H. Lee *et al.*, Phosphoproteomic analysis reveals that PP4 dephosphorylates KAP-1 impacting the DNA damage response. *EMBO J.* **31**, 2403–2415 (2012).
58. S. Hatakeyama, TRIM proteins and cancer. *Nat. Rev. Cancer* **11**, 792–804 (2011).
59. D. A. Fruman, C. Rommel, PI3K and cancer: Lessons, challenges and opportunities. *Nat. Rev. Drug Discov.* **13**, 140–156 (2014).
60. S. J. Klempner, A. P. Myers, L. C. Cantley, What a tangled web we weave: Emerging resistance mechanisms to inhibition of the phosphoinositide 3-kinase pathway. *Cancer Discov.* **3**, 1345–1354 (2013).
61. T. J. Rowland, G. Dumbović, E. P. Hass, J. L. Rinn, T. R. Cech, Single-cell imaging reveals unexpected heterogeneity of telomerase reverse transcriptase expression across human cancer cell lines. *Proc. Natl. Acad. Sci. U.S.A.* **116**, 18488–18497 (2019).